

DEVELOPMENT OF A SOLAR AIR HEATING FAÇADE

E. V. Stevenson¹, P. Jones¹, D. Alexander¹, B. Jones² and P. Jones

¹ Welsh School of Architecture, Cardiff University, Cardiff, CF10 3NB, UK

² Corus Group, ECM², Port Talbot, SA13 2EZ, UK

E-mail: StevensonV@cardiff.ac.uk

Abstract: A simple solar capture façade can be made by covering standard profiled wall elements with glass sheeting. Solar energy heats the air in the profile channels and generates air movement, while the insulated wall prevents uncontrolled heating of the building.

A mathematical model has been developed to predict the exit air temperature, air mass flow, air velocity and power output from such a system. Initial experimental work has taken place to verify the air flow component of the model. This has involved predicting the pressure drop along the length of four prototype ducts using the Darcy equation. These predictions have been found to over estimate the system pressure drop. It was found that using the Darcy equations with an adjusted hydraulic diameter (increased by 9.75%) gave a better match to the actual data for the geometries and flows considered.

Keywords: façade, heating, modelling, solar, ventilation .

1. INTRODUCTION

Finite fossil fuels resources and legislation regarding carbon emissions indicate that reduced energy consumption and alternative energy sources are required. Water heating, space heating and ventilation in buildings are major consumers of energy. Using solar air/water heating and ventilation systems would be one method of reducing carbon emissions and fossil fuel usage.

The concept of a simple solar capture façade, made from profiled steel sheeting covered with glass, is illustrated in Figure 1.

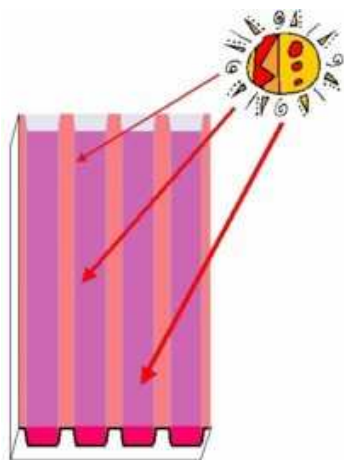


Figure 1: Concept of glazed profiled steel used as a passive solar heater

In 2003, 1400 million m² of precoated coil was sold in Europe (ECCA, 2003). Of this total, approximately 280 million m² was used in a position with potential for solar

energy capture, e.g. on roofs and south facing walls. The average insolation level for Europe has been calculated as $3.6 \text{ kWh m}^{-2} \text{ day}^{-1}$ (Whitlock and et al, 2000). Thus, annually, the solar energy falling on one year's production of precoated coil can be estimated at over 367,000 GWh. This is greater than the electricity produced from gas in the United Kingdom in a year (DTI, 2002), indicating the potential which exists for significant building integrated solar energy.

2. ENERGY BALANCE

The glass sheet covering the profiled façade effectively forms several vertical ducts. To estimate the performance of such a façade, an energy balance analysis can be carried out on an individual duct. This enables the outputs of the duct: i.e. air exit temperature (t_{ex}), mass flow rate of air (\dot{m}), velocity of air (V) and power output (P) to be calculated.

Energy enters the system as solar irradiation transmitted through the glass layer (Q_g). This can be estimated from the incident solar radiation for a location, the glazing transmission characteristic and the backing panel absorptance. Energy can leave the system through the glass, through the insulation or through the air:

1) Since glass is not a perfect insulator there will be some energy losses (Q_F) associated with the glazing, characterized by its "U-value". The calculation for Q_F is shown in equation 1 (ASHRAE, 1989):

$$Q_F = A_g U_g (t_m - t_o) \quad 1$$

2) There will also be small heat losses associated with the insulated back and sides of the duct (Q_i) determined by the backing material and degree of insulation. In this scenario Q_i is assumed to be negligible, due to backing insulation on the panel.

3) The remaining energy (Q_V) heats the air within the duct and generates air movement through solar induced stack effect. Q_V can be calculated from the resulting mass flow rate of air through the device (ASHRAE, 1989):

$$Q_V = \dot{m} C_p (t_m - t_o) \quad 2$$

An energy balance requires the energy in to equal the energy out. In this case, assuming thermal mass to be negligible:

$$Q_g = Q_F + Q_i + Q_V \quad 3$$

Substituting equations 1 and 2 into equation 3 and rearranging for \dot{m} provides an equation for air flow rate:

$$\dot{m} = \frac{Q_g - A_g U_g (t_m - t_o)}{C_p (t_m - t_o)} \quad 4$$

The air movement is a result of buoyancy. Models for the flow of heated air through a duct have been proposed by several authors (Ho and Loveday, 1997, Hollands and Shewen, 1981, Brinkworth et al., 2000). However, Brinkworth et al., (2000) have provided a model for buoyant ventilation which takes into account skin friction as well as buoyant forces. The following equation for buoyant ventilation is based on their work:

$$\dot{m}^3 = \frac{2S(\rho_o A_c)^2 gL\beta \sin \theta}{C_p \left(K_{f1} + K_{f2} + f \frac{L}{D_h} \right)} \quad 5$$

The buoyancy term (β) in equation 5 is defined in terms of the mean air temperature in the duct (t_m). The stratification parameter (S) is assumed to be 0.5 (i.e. the increase of temperature with length of duct is linear). Values for the friction coefficients are found in Brinkworth et al., (2000) and those appropriate for the system under consideration are $K_{f1} = 0.5$ and $K_{f2} = 1.0$.

Previous work (due to be published in November 2005) has confirmed that the friction factor (f) can be defined for this geometry using the following equation (ASHRAE, 1989):

$$f^* = 0.11 \left(\frac{\varepsilon}{D_h} + \frac{68}{\text{Re}} \right)^{0.25} \quad 6$$

if $f^* \geq 0.018$: $f = f^*$
 if $f^* < 0.019$: $f = 0.85 f^* + 0.0028$

The hydraulic diameter can be defined generically as (ASHRAE, 1989):

$$D_h = \frac{4A}{P} \quad 7$$

Since we are considering an air system, all four sides of the rectangular duct are wetted and included in the perimeter.

Simultaneous solution of equations 4 and 5 allows the mean air temperature and mass flow to be calculated for a given geometry and external condition. Due to the non-linearity of the terms, this solution must be determined iteratively. The exit air temperature (t_{ex}) is determined from the mean air temperature, assuming a linear variation along the length of the duct.

Once the mass flow and mean temperature are known, the air velocity can be calculated using:

$$V = \frac{\dot{m}}{A_c \rho_o} \quad 8$$

and the power generated by the system can be calculated using:

$$P = C_p \dot{m} (t_m - t_o) \quad 9$$

The mathematical model had been used to predict the likely air exit temperature and air mass flow through a variety of duct geometries in different weather conditions. From this information a matrix of promising duct geometry / length combinations was selected for experimental work. A likely spread of target air mass flows between 0.0015 and 0.025 kg s⁻¹ was selected in a similar way.

3. EXPERIMENT

The ability of these equations to predict flow and energy will depend greatly on a correct identification of the pressure losses in the system. The pressure loss of the duct will be a vital parameter in optimising the geometry of the system, as well in determining whether the system can operate as a passive collector, through buoyancy forces alone or require fan assistance. It is therefore important that the prediction of the duct pressure drop be accurate.

The aim of the experiment reported here was to verify the pressure drop calculations within the model by comparing measured and predicted pressure losses under imposed flows. Ideally the calculation of pressure drop should be applicable across a range of duct geometry, duct length and air mass flow.

Within the model already described, the pressure drop along the duct length L can be calculated using the Darcy equation (Brinkworth et al., 2000)

$$p_{fr} = f \frac{L}{D_h} \frac{\rho V^2}{2} \quad 10$$

using the symbols defined in section 2.

3.1 Experiment Equipment

Four ducts were manufactured from precoated steel. 6mm clear float glass was attached to the ducts using a silicone sealant. The dimensions of the ducts, as chosen from the prototyping procedure outlined in section 2, are shown in Table 1.

Table 1: Dimensions of Ducts

Duct ID	Width (m)	Depth (m)	Length (m)	D_h (m)
A	0.1	0.034	2.4	0.0507
B	0.1	0.0625	2.4	0.0769
C	0.15	0.033	2.4	0.0541
D	0.15	0.063	2.4	0.0887

The air was drawn through the ducts using a vacuum fan. The air flow was controlled using ball valves. The mass flow rate was calculated with an uncertainty of 1.5% from the pressure difference across an orifice plate prepared to BS EN ISO 5167-1&2:2003 (British Standards Institution, 2003a, British Standards Institution, 2003b). The experimental equipment is illustrated in Figure 2.

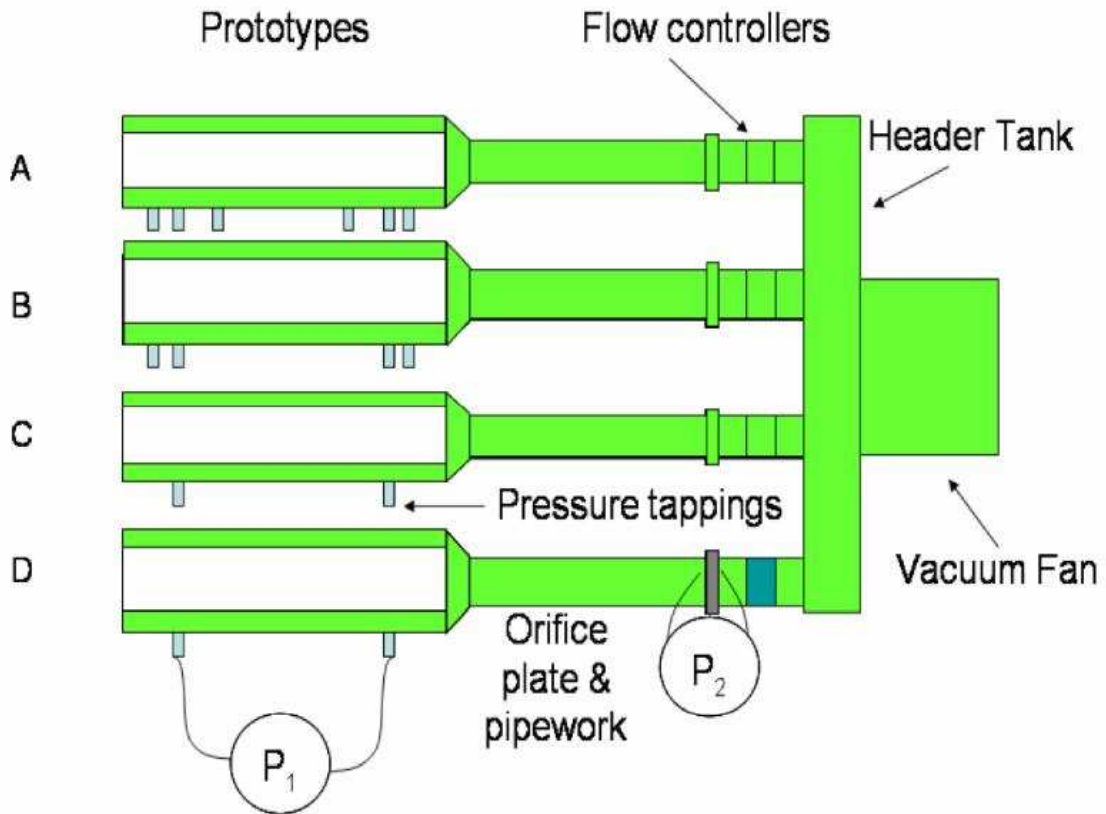


Figure 2: Schematic showing layout of experimental equipment

In order to present stable flow to the ducts, flow straighteners were placed at inlet and outlets. Although the ducts were 2m long, pressure tappings were not attached within the entry or exit areas (assumed to be less than six times the depth of the duct). Therefore all four ducts had pressure tappings attached 1.58m apart. The pressure drop across this duct length was measured, using a micro-manometer, to an accuracy of 0.1 Pa. Previous tests on ducts A and C had shown that there was a well established linear relationship between pressure drop and distance along the duct. Therefore it was considered valid to determine the duct pressure loss characteristic from a single position.

4. RESULTS AND DISCUSSION

4.1 Pressure Difference for Varying Air Mass Flow

The air mass flow through the duct will vary depending on duct geometry as well as available solar energy. Air mass flows between 0.0015 and 0.025 kg s^{-1} are expected. The pressure drop over 1.58m length was measured for all four ducts for flows within the expected range. The expected pressure drops were calculated using the Darcy Equation (equation 10). The comparison between predicted and actual pressure drops are shown in Figures 3. The repeatability was calculated by grouping data from 0.0095 to 0.0105 kg s^{-1} for 0.01 kg s^{-1} , and from 0.0175 to 0.0185 kg s^{-1} for 0.018 kg s^{-1} and calculating the root mean standard error (RMSE). The number of data points this includes and the resulting RMSE is shown in Table 2 for all four ducts. The error bars in Figure 3 indicate the variance in the actual pressure drop for each duct at these flows.

Table 2: Dimensions of Ducts

Duct ID	0.01 kg s ⁻¹ flow		0.018 kg s ⁻¹ flow	
	No of data points	RMSE (Pa)	No of data points	RMSE (Pa)
A	15	0.29	4	0.36
B	6	0.06	6	0.15
C	6	0.23	4	0.74
D	6	0.07	4	0.13

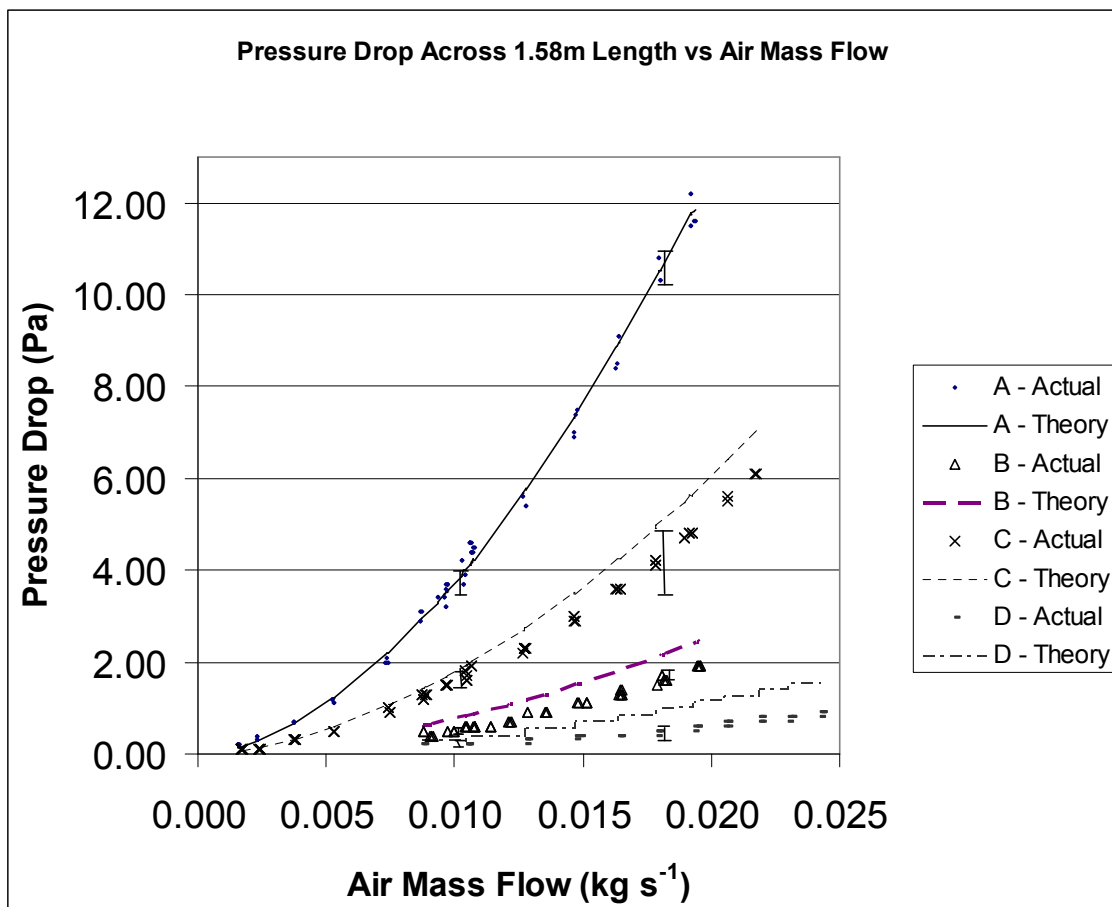


Figure 3: Relationship between pressure drop and air mass flow for 1.58m length – ducts A to D

As shown in figure 3 there is a good correlation between the pressure drop predicted using Darcy’s equation and the measured values for duct A (the smallest duct of the four tested). However, pressure drop is overestimated for ducts B, C and D. Although it is beneficial that the actual pressure loss be less than expected (so promoting greater passive flows or requiring lesser fan power), it is of interest to determine where the predictive theory is inadequate for these geometries, and where possible to tune the prediction equations.

4.2 Discussion

The flows for the four ducts had Reynolds numbers ranging between 1,000 and 18,000 – indicating that the flow is mainly transitional. Flows in this area are not well understood and there are no well established models. The Darcy equation is accepted for turbulent flow, but unproven for transitional flow. This may account for the difference between predicted and measured pressure drop values.

Potential candidates for the systematic error in the Darcy equation calculations are roughness (ϵ), friction factor (f) and hydraulic diameter (D_h). These values were varied within a reasonable limit, and the effect on the predicted values observed. Changes were assessed using mean bias and RMSE between 240 measured values and the corresponding predictions. Ideally, across the four duct geometries studied, both factors could be minimised by adjusting these parameters.

Three measurements of the surface roughness of the precoated material used in the ducts indicated a typical surface roughness of $3\mu\text{m} \pm 10\%$. The effect of varying ϵ within these limits did not make a significant difference to the pressure drop results. Therefore, it appears that ϵ is not the source of the difference between the actual and predicted pressure drops.

Table 3 shows a comparison of the mean bias (%) and RMSE (%) for the variations in f and D_h . The effect of varying f by $\pm 10\%$ was considered, from this the percentage of f which would generate the lowest bias was calculated. The bias (%) and RMSE (%) for $f - 11\%$ are shown in Table 3.

The effect of varying D_h by $\pm 10\%$ was considered, from this the percentage of D_h which would generate the lowest bias was calculated. The bias (%) and RMSE (%) for $D_h + 9.75\%$ are shown in Table 3.

For a rectangular duct, it is possible to calculate the circular equivalent diameter (D_e) as an alternative to D_h . D_e is defined as (ASHRAE, 1989), where a and b refer to the duct section dimensions:

$$D_e = 1.3 \frac{(ab)^{0.625}}{(a+b)^{0.25}} \quad 11$$

The mean bias (%) and RMSE (%) for D_e is shown in Table 3. The bias for D_e is high in comparison to the other factors considered. For this reason the effect of varying D_e by $\pm 10\%$ was considered, from this the percentage of D_e which would generate the lowest bias was calculated. The bias (%) and RMSE (%) for $D_e - 10.3\%$ are shown in Table 3.

The least bias and rms errors were achieved by either reducing f by 11% or increasing D_h by 9.75%. Since f is inversely dependent on D_h (equation 6), this is logical; it is concluded that adjusting D_h is the most appropriate tuning mechanism.

Table 3: Bias and RMSE for Factors Affecting the Darcy Equation

Ducts	Error	Darcy Equation	- 11% f	+ 9.75% D _h	D _e	-10.3% D _e
A	Mean Bias (%)	190	1,005	1,003	1,780	933
	RMSE (%)	9.3	15.4	15.4	24.5	14.7
B	Mean Bias (%)	-2,194	-1,369	-1,371	-1,234	-2,185
	RMSE (%)	42.6	27.3	27.4	24.9	42.4
C	Mean Bias (%)	-998	-162	-164	1,286	514
	RMSE (%)	19.7	11.5	11.6	21.4	12.8
D	Mean Bias (%)	-3,122	-2,240	-2,242	-1,689	-2,647
	RMSE (%)	65.4	47.6	47.6	36.5	55.8
All	Mean Bias (%)	-5,992	-31	-42	6,114	-11
	RMSE (%)	27.8	22.1	22.1	26.4	26.5

With this adjustment, the pressure drop of the ducts could be predicted to within 22% across all four duct geometries, even though the flows were in the transition region. The comparison between actual pressure drop and that predicted using $D_h + 9.75\%$ is shown in Figure 4. Agreement across all cases can now be seen. Although, at an error of 22%, the predictive power is not high, it is considered sufficient to predict system performance and to distinguish between alternative system geometries in an optimisation process.

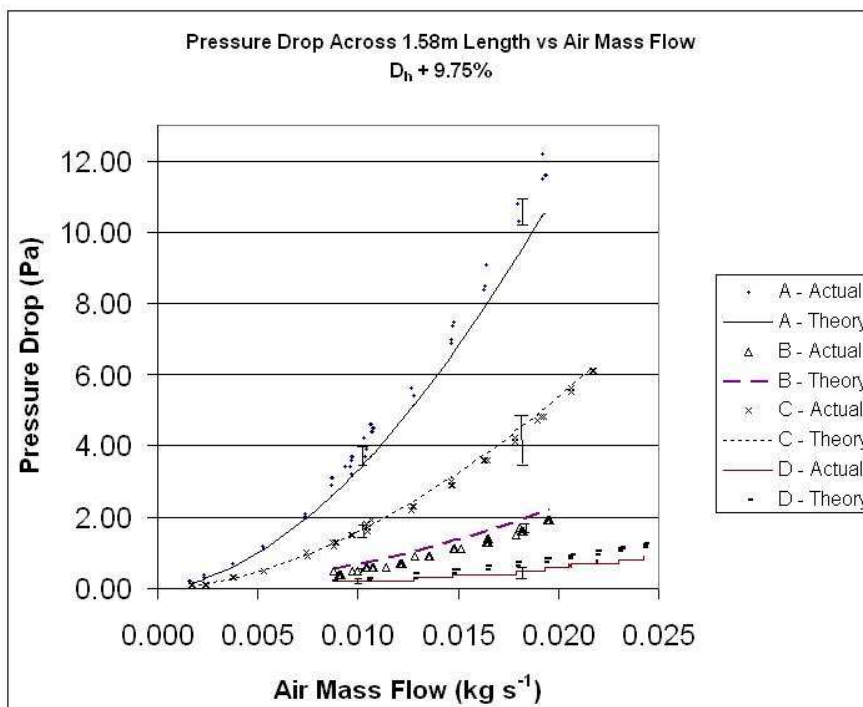


Figure 4: Relationship between pressure drop and air mass flow for 1.58m length with D_h increased by 9.75% – ducts A to D

5. CONCLUSIONS

The calculation of pressure drop due to surface friction in a prototype solar collector system was compared to measurements. For the larger duct dimensions, under the flow-rates considered, the Darcy equation was found to over estimate the system pressure drop. It was found that using the Darcy equation with an adjusted hydraulic diameter (increased by 9.75%) gave a better match to the actual data for the geometries and flows considered, reducing the mean bias as well as the rms error in the predictions. Across the range of duct geometries and flowrates considered, pressure loss due to friction could be predicted to within 22%.

The ability to predict system pressure losses will be important to a passive air heating system, since a system with a low pressure drop per metre in length is more likely to operate without the assistance of a fan.

6. NOMENCLATURE

- A_c cross-sectional area of duct (m^2)
 A_g area of glazing (m^2)
 C_p specific heat capacity of air
 D_h hydraulic diameter (m)
 f friction factor
 f' friction factor approximation
 g acceleration due to gravity
 K_{f1} pipe fitting pressure drop loss coefficient
 K_{f2} pipe fitting pressure drop loss coefficient
 L length of solar absorbing layer (m)
 \dot{m} mass flow rate of air ($kg\ s^{-1}$)
 P power output of duct (W)
 p_{fr} pressure drop due to friction (Pa)
- Q_F rate of heat transfer lost across glazing (W)
 Q_g rate of heat transfer across glazing (W)
 Q_i rate of heat transfer lost across insulation (W)
 Q_v rate of heat transfer lost through ventilation (W)
 Re Reynolds number
 S stratification parameter
 t_{ex} temperature of air exiting duct ($^{\circ}C$)
 t_m mean temperature of air in duct ($^{\circ}C$)
 t_o temperature outdoors ($^{\circ}C$)
 U_g U-value of the glazing ($W\ m^{-2}\ K^{-1}$)
 V air velocity ($m\ s^{-1}$)
 β cubic expansivity (K^{-1}) = $1/t_m(K)$

7. REFERENCES

- ASHRAE (1989) *1989 ASHRAE Handbook: Fundamentals, SI Edition*, ASHRAE, Atlanta.
- Brinkworth, B. J., Marshall, R. H. and Ibarahim, Z. (2000) *A Validated Model of Naturally Ventilated PV Cladding*, *Solar Energy*, **69**, 67-81.
- British Standards Institution, *British Standard; BS EN ISO 5167-1:2003 Measurement of fluid flow by means of pressure differential devices inserted into circular cross-section conduits running full - Part 1: General principles and requirements*. (2003a) British Standards Institution.
- British Standards Institution, *British Standard; BS EN ISO 5167-2:2003 Measurement of fluid flow by means of pressure differential devices inserted into circular cross-section conduits running full - Part 2: Orifice Plates*. (2003b) British Standards Institution.
- DTI, *Fuel used in generation*. (2002) DTI, http://www.dti.gov.uk/energy/inform/energy_stats/electricity/5_1elecfuelused-Q.xls.
- ECCA, *Statistics*. (2003) ECCA, <http://www.eccacoil.com/>.
- Ho, K. T. K. and Loveday, D. L. (1997) *Covered profiled steel cladding as an air heating solar collector: laboratory testing, modelling and validation*, *Energy and Buildings*, **26**, 293-301.
- Hollands, K. G. T. and Shewen, E. C. (1981) *Optimization of flow passage geometry for air-heating, plate-type solar collectors*, *Journal of Solar Energy Engineering*, **103**, 323-330.
- Whitlock, C. E. and et al, *Release 3 NASA Surface Meteorology and Solar Energy Data Set for Renewable Energy Industry Use. 26th Annual Conference of the Solar Energy Society of Canada, 21-24th October 2000*. (2000) Apricus, http://www.apricus-solar.com/insolation_levels_europe.htm.